❒   712

Partial Shading in Building Integrated PV System: Causes, Effects and Mitigating Techniques

Zainal Salam[1,2], Zulkifli Ramli[3], Jubaer Ahmed[1], Muhammad Amjad[4]

[1] Center of Electrical Energy Systems, Faculty of Electrical Engineering, Univeristi Teknologi Malaysia,
81310 Johor Bahru, Malaysia
[2] Insitute of Future Energy, Univeristi Teknologi Malaysia, 81310 Johor Bahru, Malaysia
[3] Faculty of Electrical Engineering, Universiti Teknikal Malaysia, Melaka, Air Keroh, Melaka, Malaysia
[4] College of Engineering and Technology, The Islamia University of Bahawalpur, Bahawalpur, Pakistan

Article Info	ABSTRACT
	This paper is aimed to provide a holistic understanding on the issues related to partial shading: its causes, the theoretical and physical reasons behind it, its implications on the BIPV system. Furthermore the possible mitigation techniques using the software (MPPT) and hardware solutions are discussed. Finally an example is given to illustrate the impact of partial shading and the economic benefits of employing various partial shading mitigation techniques into the BIPV system To aid the unfamiliar readers in this subject, a brief but comprehensive overview of important PV concepts are also given.

Corresponding Author:

Zainal Salam,
Center of Electrical Energy Systems, Faculty of Electrical Engineering,
Univeristi Teknologi Malaysia,
81310 Johor Bahru, Malaysia.
Email: zainals@fke.utm.my

1. INTRODUCTION

As a renewable source, the solar photovoltaic (PV) has attracted considerable interest for several reasons: 1) the continuous decline in the price of PV modules, 2) the mature and reliable electronic power conversion technology, 3) the simple installation process and low maintenance cost 4) environmentally friendly. In addition to these, many countries have introduced various incentive programs such as feed-in-tariff, tax breaks and initial investment rebates to accelerate the growth of this industry. In recent years, one application that has gained immense attention is the building integrated PV (BIPV) [1]. Besides provideing energy to the building, BIPV has other inherent economic potential: the modules can serve as the structural elements and reduces concentrations of added weight on roofs. In cases where the feed-in-tariff is implemented, the building can generate sufficient income to pay-back its PV investment cost—usually with sizeable profit margin.

Despite these advantages, the BIPV in urban areas faces considerable challenges—primarily due to partial shading from the taller adjacent buildings, electrical utility towers, transmission cables, telephone poles, antennas, trees etc. In many cases, the structures are not present during the planning and design stages, but are erected after the PV system has been commissioned. As a result, the BIPV has to endure the shading throughout its service lifetime. During partial shading, i.e. when one or more modules experience different irradiance than the rest of the array, the bypass diode of the module is activated, thus causing the shaded module to be bypassed. The operation causes the *P-V* curve to contain numerous maxima points with one

global peak. If the inverter is not equipped with an MPPT that could differentiate between the local and global peaks, there is a possibility for the algorithm to be trapped in one of the former, thus causing the power to drop. It is statistically reported in that the energy loss due to partial shasding can vary from 10 to 70% [2].

Despite being well-documented in literatures [3], many are not aware of the advantages that can be obtained by implementing certain partial shading mitigation measures into their BIPV system. With this hindsight in perspective, this paper discusses the causes, affects of partial shading and more importantly the strategies for its mitigation. A case study is given to illustrate the benefits of employing various partial shading mitigation techniques. It is envisaged that this work would be a valuable one-stop reference source to enable PV researchers, system designers and practitioners making more informed decisions in designing BIPV system that is subjected to partial shading.

2. SYSTEM OVERVIEW

2.1. BIPV System Configuration

The BIPV is the integration of PV cells/modules into the building envelope to become part of the structure [4]. Figure 1 shows a simplified diagram of a BIPV for a typical residential home. The modules are arranged in series strings to achieve the required working direct (dc) voltage. To increase the power, several of these strings are connected in parallel to form an array. Since most electrical appliances run on alternating (ac) voltage, the dc power extracted from the modules is converted to ac using an inverter [5].
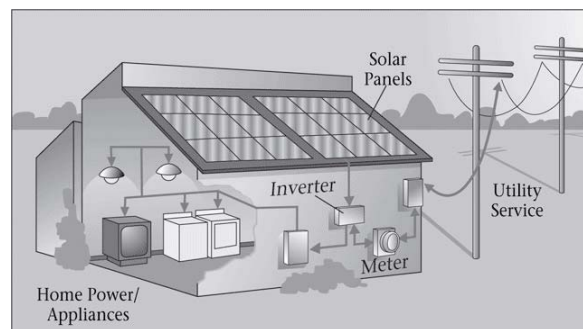
Figure 1. A Typical BIPV system configuration

2.2. The *I–V* and *P–V* Curve and MPPT

In its most basic form, a PV module (or cell) can be modelled as a current source that is dependent on the solar irradiance (G) and temperature (T). The variation in G and T results in non-linear *I–V* and *P–V* curves as shown in Figure 2(a) and (b), respectively. At any time, there exists a unique operating point, at which the power is at the peak (MPP). Due to the dynamics of G and T, a MPP tracker (MPPT) is needed to ensure maximum power is extracted from the modules under any environmental condition.

The MPPT can be categorized into the conventional and non conventional. The work in [6] have reviewed the conventional MPPT methods which include the Perturb and Observed (P&O) [7], Hill Climbing (HC) and Incremental Conductance (IC), as well as the lesser known Ripple Correlation, Open Circuit Voltage, Short Circuit Current and Sliding Control. The non-conventional MPP methods are based on soft-computing, which relies mainly on the search and optimization approach [8]-[10]. Among the conventional MPPT, the P&O is the most widely used [11]. The goal of the algorithm is to position the operating point as closest as possible to the MPP by climbing the slope of the *P-V* curve. It calculates the power (P) by sensing the voltage (V) of the PV array; then it provides a perturbation (ϕ) in V, based on the change of power, i.e.

$$X_{new} = X_{old} + \phi \times slope \quad (\text{if } P > P_{old}) \quad [\textit{Where } X = V \textit{ or } I \textit{ or } D]$$
$$X_{new} = X_{old} - \phi \times slope \quad (\text{if } P < P_{old}) \tag{1}$$

where, the slope indicates the direction of the perturbation. Clearly, the size of ϕ is crucial; if ϕ is large, the convergence is fast, but it results in large fluctuation in P and vice versa.

(a)   (b)
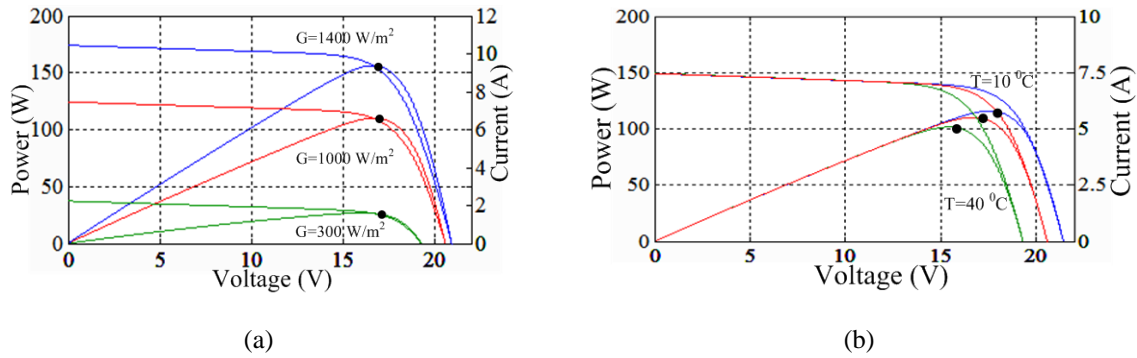
Figure 2. (a) The *I–V* and *P–V* curves under varying *G*. (b) *I–V* and *P–V* curves under different *T*

3.   PV CHARACTERISTICS DURING PARTIAL SHADING

3.1. Partial Shading Phenomena

In BIPV, the main cause of partial shading is the obstructions from the surrounding buildings, and other tall structures such as trees, telephone pole, transmission lines and antennas. Partial shading-like characteristics is also exhibited by module irregularities such as cracks. Practically, every module is fitted with a bypass diode to avoid a hot spot (i.e. concentration of current into one module) if any of the module is shaded. When the entire PV string experience a uniform irradiance (which is the normal condition), the bypass diode remains off due to the equipotential across its terminals. In this case, the *P–V* curve exhibits the normal single peak characteristics, as shown by Curve (1) of Figure 3(c). When partial shading occurs, the potential difference triggers the bypass diode, causing the current to be diverted away from the shaded module. Since the shaded module is short circuited, the voltage across it ceases to zero. Consequently, the *P–V* curve is characterized by several local and a global peak, as illustrated by Curve (2). A good MPPT is expected track the global, while avoiding any of the local peak.. Unfortunately, for the conventional MPPT (such as P&O), once it locates a particular peak (regardless whether it is global or local), the algorithm forces the operating point to go forth and backwards around the perceived MPP, causing power loss.
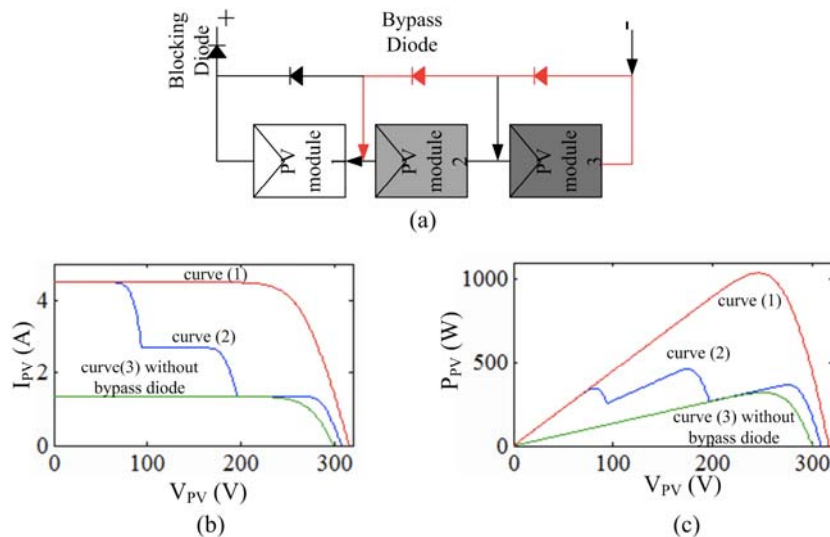
Figure 3 (a) PV under patial shading (b) the resulting *I–V* (c) *P–V* curve

4.   PARTIAL SHADING MITIGATION

To mitigate the effect of partial shading, three approaches are possible. First is by by adding more intelligence to the P&O to enable it to differentiate between the local and global peak. Alternatively, soft computing techniques can be utilized to scan the entire (or part of the) PV curve in order to locate the global peak. In both cases, only modifications in the software, i.e. the MPPT codes are necessary. The second

approach is to retrofit the inverter/converter with dedicated energy recovery circuit to harvest whatever energy is available from the shaded modules. It ensures that power from the shaded module is utilized by balancing the total current that flow into the PV string. The third approach is to fit a small inverter to each module, known as the micro-inverter. In this method, the central inverter is no longer required because every micro-inverter is individually connected directly to the grid.

4.1. Modified P&O

Patel & Agarwal [12] proposed a two-mode modified P&O that divides the MPP tracking into main parts: the global and the local tracking mode. The former is used to bring the operating point to the vicinity of the global peak, while the latter is designed to maintain the operating point once the global peak is detected. To avoid the scanning of the entire voltage span, two critical steps are taken: 1) the peaks are assumed to be at the multiples of 80% of V_{oc} and 2) the minimum displacement between successive peaks is approximately 80% of V_{oc}. Furtheremoe, the detection of the partial shading is triggered by a threshold value ΔP_{crit}. If the power change is larger than ΔP_{crit} then partial shading is assumed to have occurred, prompting algorithm to jump into the global mode. Once within the vicinity of the global peak, the algorithm switches over to the local mode, which is the conventional P&O. It stays there until a new partial shading condition is detected. Similar tracking method is also presented in [13]. However, unlike the duty cycle is utilized as the main control variable; thus it can be categorized as the hill climbing. In another work [14], the P&O is replaced by the IC to perform the search mechanism, while the procedure to distinguish between local and global peak is similar to [13].

4.2. Soft Computing

Soft computing is an optimization technique that exhibits natural ability to search for minima/minima points [15]. Depending on the algorithm, it performs a search for the global peak over the entire span (0 to V_{oc}) or only certain sections of voltage range. Salam *et. al.* [8] and Ishaque *et. al.* [10] have summarized the soft computing MPPT which include Artificial Neural Network (ANN) [16], Fuzzy Logic [17] and Particle Swarm Optimization (PSO) [18],[19], Differential Evolution (DE) [20]. More recently the Ant Colony Optimization (ACO) [21] and Chaotic Search [22], Cuckoo Search [23] have also been used to handle the partial shading condition. However, since many of the method pursue similar processes, only one method, namely PSO is considered.

In PSO, a number of particles roam within the search-space according to their position and movement velocity [24]. The idea is depicted by Figure 4; the position of each particle is determined by its own best position and the global best positions. The position of the individual particle is given by

$$x_i^{k+1} = x_i^k + v_i^{k+1} \tag{2}$$

where v_i corresponds to the velocity component. It is calculated by using the following relationship:

$$v_i^{k+1} = wv_i^k + c_1 r_1 (P_{best} - x_i^k) + c_2 r_2 (G_{best} - x_i^k) \tag{3}$$

In (3), w is the inertia weight, c_1 and c_2 are the acceleration constants, while P_{best} and G_{best} are the personal and global best positions, respectively. To start the optimization process, a vector of duty cycles are initialized and the algorithm transmits the duty cycles to the power converter. These duty cycles (represented by x_i in (2) serve as the initial particles in the first iteration. All particles are heading towards their local best position P_{best}. Among these particles, one of them is the global best G_{best}. It gives the best fitness value. After calculating the velocity, which serves as a perturbation to the voltage, a new position of the voltage is found. Through successive iteration all particles move towards global best position. As the particles approach the MPP, they get closer to the G_{best} position. Correspondingly, the P_{best} factor and G_{best} factor in velocity term moves towards zero. Eventually a zero velocity is achieved and the voltage position remains almost unchanged. Under this condition, the PV system reaches at MPP.
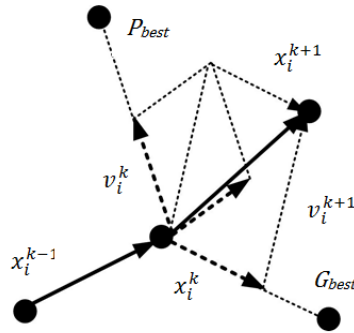
Figure 4. Movement of Particles in PSO

To compare the performance of the conventional P&O and PSO during partial shading, a scenario involving fourn series-connected PV modules, labelled as A, B, C and D is simulated. The specifications of the modules at the Standard Test Condition[1] (STC) of the are given in Table 1. The simulation is carried out using the simulator developed by [25], which utilizes the two-diode model for the solar cel. Initially each module receives an uniform irradiance of 1000W/m^2. Consequently, there exists only one MPP at 440 W, as shown by Curve 1 of Figure 5(a). After a lapse of one second, modules A, B, C and D are irradiated with 1000 W/m^2, 800 W/m^2, 500 W/m^2 and 300 W/m^2 respectively. Due to these partial shadings, multiple peaks are generated in the *P–V* curve, as shown by Curve 2 of the same figure. These are 115 W, 220 W, 280 W and 240 W. As the operating point shifts from Curve 1 to Curve 2, the P&O algorithm will climb to the nearest peak, i.e. 240 W as directed by the arrows in Figure 5(a). Clearly, this peak is local. However, in the case of PSO, when partial shading is detected, the algorithm begins the search for the global peak. After successive iterations, the global MPP (i.e. 280 W) is tracked, as directed by the particles movements (using the direction of arrow) in Figure 5(b). The difference between the global and local peak is 40 W, or approximately 14% of the peak power. In the context of PV system, such power loss is considered very significant. The output power timing diagrams for both cases are shown in Figure 6. As can be observed, at the point of partial shading occurrence (at one second), the P&O quickly get trapped at the local peak, i.e. 240 W. On the other hand PSO successfully tracks the global MPP at 280 W. This result is consistent with the observation of the *P–V* curve in Figure 5(a) and (b), respectively.

Table 1. Module specifications at Standard Test Condition (STC)

Parameters	Symbol	Value
Power at MPP	P_{MPP}	110 W
Voltage at MPP	V_{MPP}	16.7 V
Current at MPP	I_{MPP}	6.6 A
Open circuit voltage	V_{OC}	20.7 V
Short circuit current	I_{SC}	7.5 A

(a)   (b)
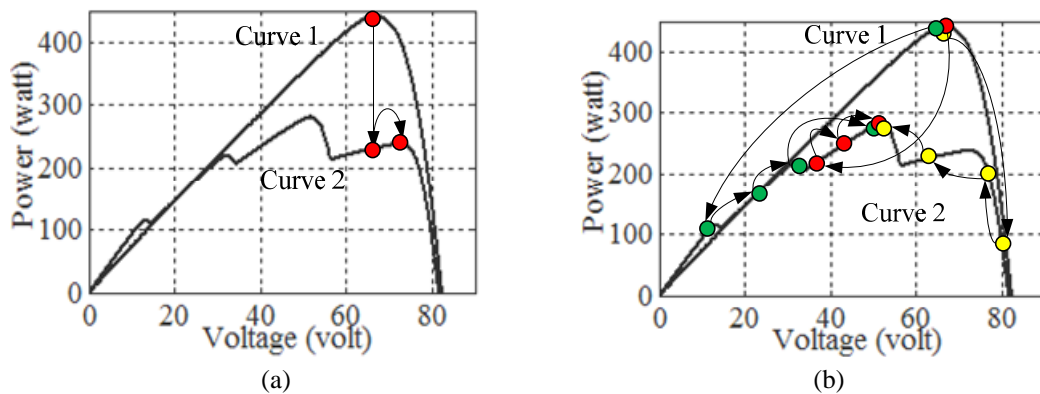
Figure 5. *P–V* curve for MPP tracking under partial shading (a) Conventional P&O (b) PSO

---

[1] Standard Test Condition (STC): Irradiance: 1000 w/m^2, Temperature= 25°C, Pressure=1 ATM.
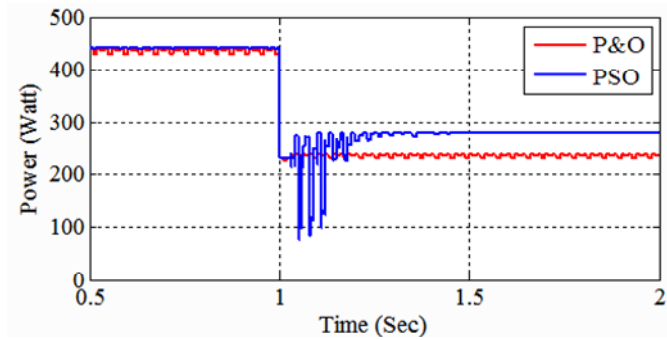
Figure 6. MPP tracking by PSO and P&O under partial shading

4.3. Energy Recovery Circuit

Although the modified P&O and soft computing MPPT are able to track the global peak, it must be noted that as long as the shaded module is being short-circuited by the bypass diode, that particular module is totally unusable. This is despite the fact that the module receives certain amount of energy while it is shaded. To make the shaded module usable, the energy recovery circuit is proposed [26],[27]. The idea is to capture the energy from the non-shaded modules and then share it with the shaded module until the power delivered by each module in the string is balanced. The circuit can be easily retrofitted to the central inverter system with minimum changes in the electrical wirings. Typically bidirectional buck-boost, flyback or cuk converter is used. There are several variations [28], but the concept remains as illustrated in Figure 7(a).

The operation of the energy recovery circuit is shown in Figure 7(b). The basic unit comprises of four modules, which is divided into two groups. Group 1 involves PV1 and PV2, together with their corresponding power electronics circuit, comprises of S_1, D_1, L_1, C_1, S_2, D_2 and C_2. Group 2 includes PV3, PV4 with S_3, S_4, D_3, D_4, L_2, C_3 and C_4. In order to connect the two groups together, the capacitor C_5 is used. Assuming that PV1 is shaded and PV2 receives full irradiation, PV2 delivers higher current than PV1. However, since the modules are connected in series, the string current will be limited to the amount delivered by PV1. During partial shading, part of the current from PV2 is diverted to the energy recovery circuit (by turning S_2 on) and the energy is stored temporarily in L_1. By doing so, the string current can be maintained at the level generated by PV1 and hence there is no need for PV1 to be bypassed. As a result, PV1 is still able to actively producing power (albeit in lesser amount, depending on the shading condition) because its voltage is not zero. Meanwhile, the energy stored in L_1 will be released back to the output via D_1 (by turning off S_2). Thus, no PV power is wasted except for the non-idealities in active and the passive components.

(a)   (b)
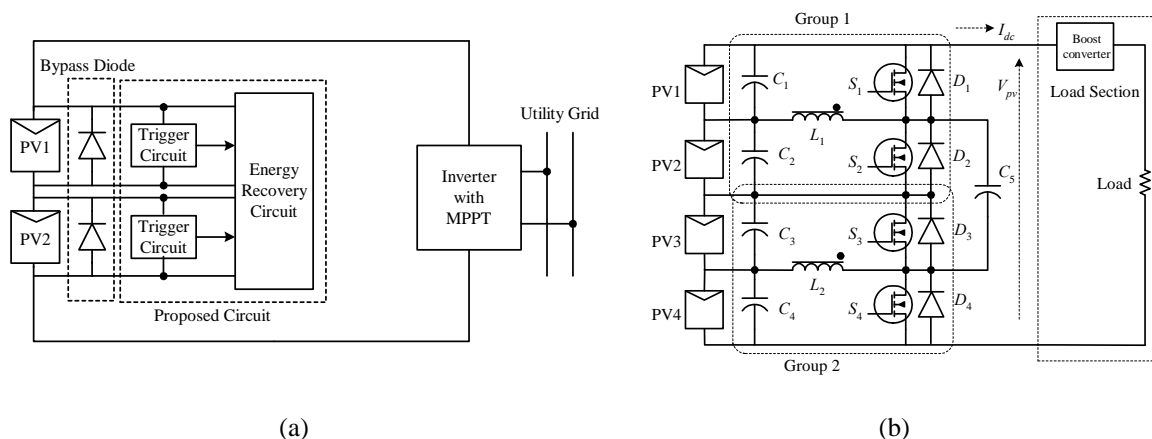
Figure 7. (a) The overall block diagram of the energy recovery circuit. (b) Detail of the energy recovery circuit

4.4. Micro-inverter

The concept is totally different from the energy recovery circuit because it does not utilised a central inverter [29]. Instead, small dedicated inverters are directly connected to the ac grid [30], as shown in Figure 8. This configuration is very attractive for low voltage grid, which particularly suits the residential BIPV. Each inverter is equipped with its own MPPT controller; thus the output from the inverter can be controlled independently. For example, if PV1 is shaded, other modules are not affected by because they are not connected as one string. Despite its attractiveness, during normal operation, the inverter conducts the full load current, resulting in high conduction and switching losses. Furthermore, the reliability of the electronics components is reduced due to their exposure to harsh environment conditions, particularly high operating temperature. For a large system with high number of modules, the cost of inverters, wiring and the complexity of the system increases very rapidly.
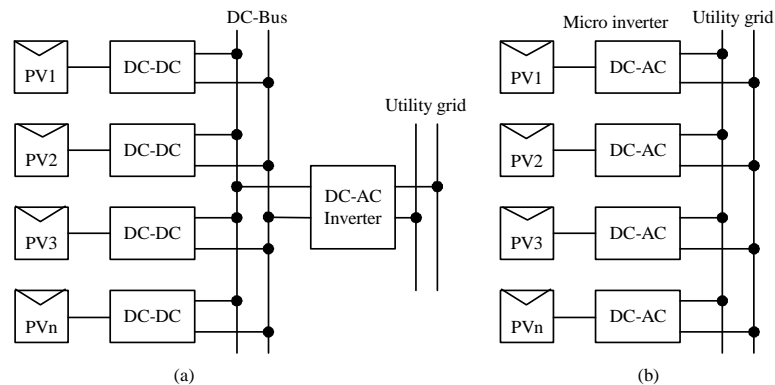
Figure 8. Micro inverter interconnection

5.   CASE STUDY
5.1. BIPV System set-up

A simulation of a BIPV system is carried out using software developed by [25]. The set-up is a two-string PV array comprises of 16 modules, configured by eight modules per string. The module has the foloowing STC specifications: P_{MPP} = 240 W, V_{MPP} = 19.08 V, I_{MPP}= 8.22 A, V_{OC} =37.25 V and I_{SC} = 8.28 A. Based on these data, the theoretical output power of the system is 3.80 kWp (i.e. 16×240 W). To quantify the effect of partial shading, six arbitrarily shading patterns are imposed, as shown in Table 2; they are labelled as conditions PS1 through PS5. In the first column, the "no-shading" is given as the benchmark. Furthermore, for simplicity, several logical assumptions are made: 1) only four irradiation values, i.e. 1.0, 0.7, 0.5 and 0.25 kW/m^2 are used to represent the different levels of shading intensities, 2) the shadings are assumed to be consistent (in terms of intensity and time profile), 3) the power electronics circuits are assumed to be 100% efficient and 4) the module temperature is uniformly taken to be constant, i.e. at 40° C. As an example, Figure 9 shows the module-inverter connection for condition PS5. The corresponding P-V curve is shown in Figure 9(b). It exhibits three peaks, namely P1, P2, P3, with P3 being the global. On the other hand, when the energy recovery method is applied, the multiple peak curve is transformed into a single peak. Clearly, it has an advantage because the peak power is higher. For the micro-inverter, the direct connection of all sixteen inverters to the grid is made similar to Figure 9. The total power available is the sum of power harvested by the individual micro-inverter from its respective module.

5.2. Results

The results are shown in Table 3. For the non-shading condition, the generated power is lower than the theoretical value, i.e. 3.16 kW (instead of 3.80 kW). This is expected as the modules are subjected to a higher temperature (40°C), while the specification in TABLE II is at STC (25°C). Furthermore, for simplicity it is assumed that the power harvested by each mitigation method with the absence of shading (benchmark case) is equal to the conventional P&O. For the modified P&O as well as the soft computing method, since the P-V curve exhibits a unique MPP, the algorithm should track the same value.

The first row of Table 3 shows the harvested power using the conventional P&O. Depending on the location of MPP prior to the partial shading occurrence, the transition of the operating point from the single peak to the multi peak curve results in one the following possibilities: the P&O algorithm finds itself located

at the 1) global peak, 2) the lowest peak, or 3) at one of the peak in-between the global and the lowest. For example, in Figure 9(b), it could be P1, P2 or P3, respectively. In this study, the selected operating point is the lowest among the available peaks. Consequently, for the conventional P&O, the results shown in the table are considered as the worst case. If $P_{no\_shading}$ is the power generated by the PV system when shading is absent, while P_{with_shade} is the power generated when a particular shading pattern is imposed, then the power loss is computed by

$$P_{loss} = P_{no\_shade} - P_{with\_shade}$$

      The loss due to partial shading varies according to the shading conditions and the mitigation approach. For instance, with the absence of mitigation, for condition PS1 (with only two modules shaded), the power loss is approximately 17%. In the case of PS5 (with 10 modules shaded), the loss increases to over 73%. However, by observing the table, there is no straightforward mathematical relationship between the shading pattern and the output power. Furthermore, the losses could not be easily quantified due to the infinite possibilities for the shading pattern. Despite this fact, the effectiveness of the mitigation can be generalized in the following order: the best efficiency is obtained using the micro-inverter, followed by the energy recovery circuit, then the modified P&O or soft computing. The performance of micro-inverter is to be expected because each inverter is able to harvest the energy from the individual module—even if the module is shaded.

Table 2. The shading patterns imposed on the modules. Note: For benchmarking, no shading is imposed.

Module Number/ Condition	No Shading (bench-marking)	Irradiation for shading conditions (kW/m^2)				
		PS1	PS2	PS3	PS4	PS5
PV1, PV9	1.00	1.00	1.00	0.25	0.70	0.25
PV2, PV10	1.00	1.00	1.00	0.25	1.00	0.25
PV3, PV11	1.00	1.00	1.00	0.50	1.00	0.25
PV4, PV12	1.00	0.70	0.25	0.70	1.00	1.00
PV5, PV13	1.00	1.00	0.25	1.00	0.70	1.00
PV6, PV14	1.00	1.00	1.00	1.00	0.50	0.50
PV7, PV15	1.00	1.00	1.00	1.00	0.50	0.50
PV8, PV16	1.00	1.00	1.00	1.00	1.00	1.00

(a)   (b)
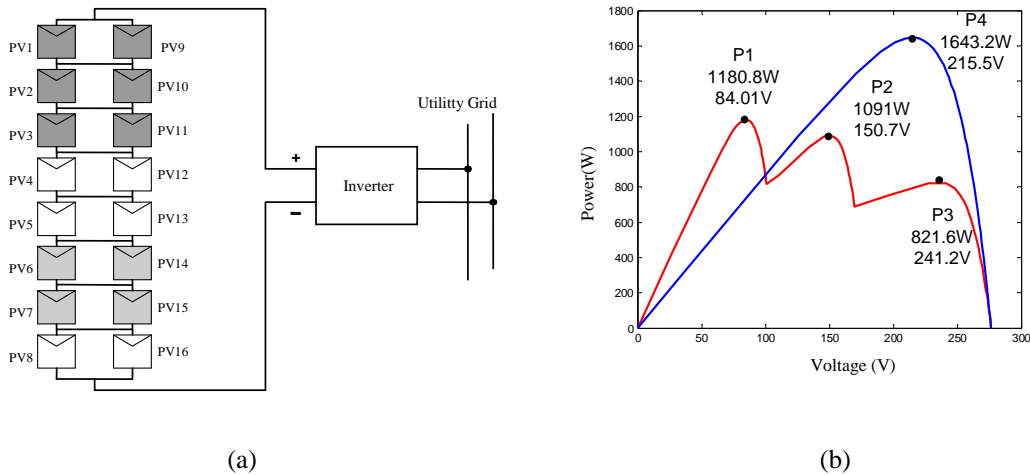
Figure 9. (a) Shading pattern PS5, (b) Its corresponding *P-V* curve. Red trace: for the MPPT algortith to track the global peak. Blue trace: curve resulting from the energy recovery circuit.

Table 3. The performance of various mitigation methods under different shading patterns. The power generated without shding is 3.16 kW.

Methods/ Shading Pattern	Shading Pattern: PS1			Shading Pattern: PS2			Shading Pattern: PS3			Shading Pattern: PS4			Shading Pattern: PS5		
	Pwr Gen. (kW)	Pwr Loss (Pl$_{oss}$)		Pwr Gen. (kW)	Pwr Loss (Pl$_{oss}$)		Pwr Gen. (kW)	Pwr Loss (Pl$_{oss}$)		Pwr Gen. (kW)	Pwr Loss (Pl$_{oss}$)		Pwr Gen. (kW)	Pwr Loss (Pl$_{oss}$)	
		kW	%		kW	%		kW	%		kW	%		kW	%
Convention al P&O MPP	2.61	0.54	17.2	0.91	2.25	71.2	0.89	2.27	71.8	1.18	1.98	62.6	0.82	2.33	73.4
Modified P&O/Soft Computing MPPT	2.75	0.41	12.8	2.36	0.80	25.2	1.59	1.56	49.5	1.72	1.43	45.5	1.18	1.97	62.6
Energy Recovery Circuit	2.91	0.25	7.8	2.41	0.74	23.5	2.05	1.10	35.0	2.27	0.88	28.0	1.64	1.51	47.9
Micro-inverter	3.02	0.13	4.3	2.52	0.64	20.1	2.19	0.97	30.7	2.48	0.68	21.5	1.79	1.36	43.2

6. CONCLUSION

Having done all these analysis, it should be realized that the energy recovery circuit requires additional hardware to be fitted into the existing PV system. Currently, the real cost of this hardware is unknown because most of the prototypes are only available in the research labs. Despite this fact, looking into the prospect, it is likely that these ideas would be translated into commercial product soon. For the case of micro-inverter, the total cost for the sixteen inverter units (and their BOS components) might be higher than one central inverter. Furthermore, the micro-inverter is relatively new, while the central inverter has been dominating the market for some time. However, as with other technology, as the volume of the micro-inverter grows, the price will drop. Moreover, it has to be realized that PV system is a long term investment. Thus the final decision to install additional hardware can be justified by taking into account the long term profitability.

REFERENCES

[1] DHW. Li, SKH. Chow, EWM. Lee, "An analysis of a medium size grid-connected building integrated photovoltaic (BIPV) system using measured data", *Energy and Buildings,* vol. 60, pp. 383-387, 2013.

[2] CR. Sullivan, J. Awerbuch, AM. Latham, "Decrease in photovoltaic power output from ripple: Simple general calculation and effect of partial shading", Applied Power Electronics Conference and Exposition (APEC), 2011 Twenty-Sixth Annual IEEE, pp. 1954-1960, 2011.

[3] YJ. Wang, PC. Hsu, "An investigation on partial shading of PV modules with different connection configurations of PV cells", *Energy,* vol. 36, pp. 3069-3078, 2011.

[4] C. Peng, Y. Huang, Z. Wu, "Building-integrated photovoltaics (BIPV) in architectural design in China", *Energy and Buildings,* vol/issue: 43(12), pp. 3592-3598, 2011.

[5] M. Yamaguchi, T. Takamoto, K. Araki, N. Ekins-Daukes, "Multi-junction III–V solar cells: current status and future potential", *Solar Energy,* vol. 79, pp. 78-85, 2005.

[6] T. Esram, PL. Chapman, "Comparison of Photovoltaic Array Maximum Power Point Tracking Techniques", *Energy Conversion, IEEE Transactions on,* vol. 22, pp. 439-449, 2007.

[7] J. Ahmed, Z. Salam, "An improved perturb and observe (P&O) maximum power point tracking (MPPT) algorithm for higher efficiency", *Applied Energy,* vol. 150, pp. 97-108, 2015.

[8] Z. Salam, J. Ahmed, BS. Merugu, "The application of soft computing methods for MPPT of PV system: A technological and status review", *Applied Energy,* vol. 107, pp. 135-148, 2013.

[9] J. Ahmed, Z. Salam, "A critical evaluation on maximum power point tracking methods for partial shading in PV systems", *Renewable and Sustainable Energy Reviews,* vol. 47, pp. 933-953, 2015.

[10] K. Ishaque, Z. Salam, "A review of maximum power point tracking techniques of PV system for uniform insolation and partial shading condition", *Renewable and Sustainable Energy Rev,* vol/issue: 19(3), pp. 475-488, 2013.

[11] N. Femia, G. Petrone, G. Spagnuolo, M. Vitelli, "A technique for improving P&O MPPT performances of double-stage grid-connected photovoltaic systems", *Ind. Electr. IEEE Trans.* vol. 56, pp. 4473-4482, 2009.

[12] H. Patel, V. Agarwal, "Maximum Power Point Tracking Scheme for PV Systems Operating Under Partially Shaded Conditions", *Industrial Electronics, IEEE Transactions on,* vol. 55, pp. 1689-1698, 2008.

[13] A. Kouchaki, H. Iman-Eini, B. Asaei, "A new maximum power point tracking strategy for PV arrays under uniform and non-uniform insolation conditions", *Solar Energy,* vol. 91, pp. 221-232, 2013.

[14] K. Punitha, D. Devaraj, S. Sakthivel, "Artificial neural network based modified incremental conductance algorithm for maximum power point tracking in photovoltaic system under partial shading conditions", *Energy,* vol. 62, pp. 330-340, 2013.

[15] PP. Bonissone, "Soft computing: the convergence of emerging reasoning technologies", *Soft Computing,* vol. 1, pp. 6-18, 1997.

[16] AZ. Alabedin, E. El-Saadany, M. Salama, "Maximum power point tracking for Photovoltaic systems using fuzzy logic and artificial neural networks", Power and Energy Soc. General Meeting, 2011 IEEE, pp. 1-9, 2011.

[17] S. Subiyanto, A. Mohamed, MA. Hannan, "Intelligent maximum power point tracking for PV system using Hopfield neural network optimized fuzzy logic controller", *Energy and Buildings,* vol. 51, pp. 29-38, 2012.

[18] K. Ishaque, Z. Salam, M. Amjad, S. Mekhilef, "An Improved Particle Swarm Optimization (PSO)–Based MPPT for PV With Reduced Steady-State Oscillation", *Pwr Elect., IEEE Trans.* vol. 27, pp. 3627-3638, 2012.

[19] K. Ishaque, Z. Salam, "A Deterministic Particle Swarm Optimization Maximum Power Point Tracker for Photovoltaic System Under Partial Shading Condition", *Ind, Electr,, IEEE Trans,* vol. 60, pp. 3195-3206, 2013.

[20] MFN. Tajuddin, SM. Ayob, Z. Salam, MS. Saad, "Evolutionary based maximum power point tracking technique using differential evolution algorithm", *Energy and Buildings,* vol. 67, pp. 245-252, 2013.

[21] LL. Jiang, DL. Maskell, JC. Patra, "A novel ant colony optimization-based maximum power point tracking for photovoltaic systems under partially shaded conditions", *Energy and Buildings,* vol. 58, pp. 227-236, 2013.

[22] Z. Lin, C. Yan, G. Ke, J. Fangcheng, "New Approach for MPPT Control of Photovoltaic System With Mutative-Scale Dual-Carrier Chaotic Search", *Power Electronics, IEEE Trans. on,* vol. 26, pp. 1038-1048, 2011.

[23] J. Ahmed, Z. Salam, "A Maximum Power Point Tracking (MPPT) for PV system using Cuckoo Search with partial shading capability", *Applied Energy,* vol. 119, pp. 118-130, 2014.

[24] JJ. Soon, KS. Low, "Photovoltaic model identification using particle swarm optimization with inverse barrier constraint", *Power Electronics, IEEE Transactions on,* vol. 27, pp. 3975-3983, 2012.

[25] K. Ishaque, Z. Salam, H. Taheri, Syafaruddin, "Modeling and simulation of photovoltaic (PV) system during partial shading based on a two-diode model", *Simul. Modelling Practice and Theory,* vol. 19, pp. 1613-1626, 2011.

[26] W. Yanzhi, L. Xue, K. Younghyun, C. Naehyuck, M. Pedram, "Enhancing efficiency and robustness of a photovoltaic power system under partial shading", Quality Electronic Design, 2012 13th International Symposium on, pp. 592-600, 2012.

[27] M. Z. Ramli, Z. Salam, "A Simple Energy Recovery Scheme to Harvest the Energy from Shaded Photovoltaic Modules During Partial Shading", *Power Electronics, IEEE Transactions on,* vol. 29, pp. 6458-6471, 2014.

[28] T. Shimizu, O. Hashimoto, G. Kimura, "A novel high-performance utility-interactive photovoltaic inverter system", *Power Electronics, IEEE Transactions on,* vol. 18, pp. 704-711, 2003.

[29] MB. Kalashani, M. Farsadi, "New Structure for Photovoltaic Systems with Maximum Power Point Tracking Ability", *International Journal of Power Electronics and Drive Systems (IJPEDS),* vol. 4, pp. 489-498, 2014.

[30] R. Orduz, J. Solórzano, M. Á. Egido, E. Roman, "Analytical study and evaluation results of power optimizers for distributed power conditioning in photovoltaic arrays", *Progress in Photovoltaics: Research and Applications,* 2011.

BIOGRAPHIES OF AUTHORS

Zainal Salam received the B.Sc. degree in electronics engineering from the California State University, Chico, CA, USA, the M.E.E. degree in electrical engineering from the Universiti Teknologi Malaysia (UTM), Johor Bahru, Malaysia, and the Ph.D. degree in power electronics, from the University of Birmingham, Birmingham, U.K., in 1985,1989, and 1997, respectively. He is currently the Professor in power electronics and renewable energy at the Faculty of Electrical Engineering UTM.. Since 2011, he has been the Editor of IEEE Trans. Sust. Energy. He represents the country as the expert for the International Energy Agency (IEA) PV Power Systems Task 13 Working Group, which focuses on the reliability and performance of the PV power system.

Mohd. Zulkifli Ramli was born in Terengganu, Malaysia in 1978. He received the B.Sc. and M.Eng. degrees from the Universiti Teknologi Malaysia (UTM), Johor Bahru, Malaysia, in 2000 and 2004,respectively, all in electrical engineering. He is currently working toward the Ph.D. degree at UTM in the area of photovoltaic. He is currently a Senior Lecturer at the Universiti TeknikalMelaka, Melaka, Malaysia. His primary research interests include the hardware design of all power converters and their control systems.

Jubaer Ahmed received the B.Sc. degree in Electrical and Electronics Engineering from Bangladesh University of Engineering and Technology (BUET), Bangladesh. Currently he is conducting his PhD in Universiti Teknologi Malaysia (UTM), Johor Bahru, Malaysia. His research interests include photovoltaic modeling and control, energy conversion from renewable sources and power electronics.

Muhammad Amjad received the B.Sc. and M.Sc. and PhD degrees in electrical engineering from the University of Engineering and Technology, Lahore, Pakistan and Universiti Teknologi Malaysia in 1998 and 2006, and 2014 respectively. He is now an Associate Professor with the College of Engineering and Technology, The Islamia University of Bahawalpur, Bahawalpur, Pakistan. His research interests include modeling of dielectric barrier discharge (DBD) chambers and power electronic converters for DBD applications.